AVT and IT regulate ion transport across the opercular epithelium of killifish (*Fundulus heteroclitus*) and gilthead sea bream (*Sparus aurata*)

Juan Antonio Martos-Sitcha[1,2,3], Gonzalo MartínezRodríguez[2], Juan Miguel Mancera[3] and Juan Fuentes[1]

(1) Centre of Marine Sciences (CCMar), Universidade do Algarve, Campus de Gambelas, 8005-139 Faro, Portugal

(2) Instituto de Ciencias Marinas de Andalucía, Consejo Superior Investigaciones Científicas (ICMAN-CSIC), E-11510 Puerto Real (Cádiz), Spain.

(3) Departamento de Biología, Facultad de Ciencias del Mar y Ambientales, Universidad de Cádiz, E-11510 Puerto Real (Cádiz), Spain.

Running head title: AVT and IT effects in marine fish operculum

Author for correspondence:
Juan Fuentes (jfuentes@ualg.pt)
Centre of Marine Sciences (CCMar),
Universidade do Algarve
Campus de Gambelas,
Building 8, Room 2.81
8005-139 Faro, Portugal

☏ +351289800900 X 7375 (Office)

☏ +351289800900 X 7134 (Lab)

ABSTRACT

The regulatory role of arginine vasotocin (AVT) and isotocin (IT) in Cl^- secretion was investigated with the short-circuit current (Isc) technique in opercular epithelia of killifish (*Fundulus heteroclitus*) and gilthead sea bream (*Sparus aurata*). Sea bream operculum showed ~4 fold lower number of Na/K-ATPase immunoreactive cells and ~12 fold lower secretory current than the killifish. In sea bream opercular membranes, basolateral addition of AVT (10^{-6} M) significantly stimulated Cl^- secretion, while IT (10^{-6} M) was without effect. In killifish, IT produced an immediate dose-dependent stimulation of Cl^- secretion with significant effect at doses $\geq 10^{-7}$ M and stimulation maxima (ΔIsc ~25 $\mu A.cm^{-2}$) at 10^{-6} M. Basolateral addition of bumetanide (200 µM) abolished >75% of the effect of IT on Cl^- secretion. In turn, AVT had a dual effect on killifish opercular Isc: an immediate response (~3 min) with Isc reduction in an inverted bell-shaped dose-response manner with higher current decrease (-22 $\mu A.cm^{-2}$) at 10^{-8} M AVT, and a sustained dose-dependent stimulation of Cl^- secretion (stable up to 1 h), with a threshold significant effect at 10^{-8} M and maximal stimulation (~20 $\mu A.cm^{-2}$) at 10^{-6} M. Both effects of AVT appear receptor-type-specific. The V1-receptor antagonist SR 49059 abolished Isc reduction in response to AVT; while the specific V2-receptor antagonist (Tolvaptan, 1 µM) abolished the stimulatory action of AVT on Cl^- secretion. According to these results, we propose a modulatory role for AVT and IT in Cl^- (NaCl) secretion across the opercular epithelium of marine teleost.

Keywords: *Fundulus heteroclitus*, ion transport, isotocin, operculum, *Sparus aurata*, vasotocin.

INTRODUCTION

Arginine vasotocin (AVT) and isotocin (IT) are typical neurohypophysial hormones in non-mammalian vertebrates (Acher, 1993). They are pleiotropic hormones with endocrine effects related to different physiological processes: osmoregulation, control of blood pressure/cardiovascular activity, metabolism, stress, reproductive behavior, brain neurotransmission and pituitary endocrine activity (Balment et al., 2006; Kulczykowska, 2007; Warne et al., 2002). Similar to other groups such as mammals (Boselt et al., 2009; Thibonnier et al., 1994), birds or amphibians (Cornett et al., 2003; Hasunuma et al., 2010; Jurkevich et al., 2005; Tan et al., 2000), different types of AVT receptors have been described in teleosts at mRNA (Conklin et al., 1999; Konno et al., 2009; Lema et al., 2012; Mahlmann et al., 1994) or genomic (Daza et al., 2012; Yamaguchi et al., 2012) levels. Two distinct AVR receptor subtypes V1a paralogs (V1a1 and V1a2) and a previously unknown V2 receptor have been, for example, identified in *Cyprimodon nevadensis amargosae* (Lema, 2010), *Oryzias latipes* (acc. no. AB539139) or *Amphiprion ocellaris* (acc. no. AB669617). While only a single IT receptor (ITR) has been reported in fish in the literature (Hausmann et al., 1995; Lema, 2010) recent evidence suggests the presence of two different ITR mRNAs in *Oryzias latipes* (ITR1: acc. no. AB646240; ITR2: acc. no. AB646241) and *Stegastes partitus* (ITR1: acc. no. JX051871; ITR2: acc. no. JX051872). In the sea bream *Sparus aurata*, two different AVTR (the V1a2-type receptor, and the V2-type receptor) as well as a single ITR have been reported (Martos-Sitcha et al., 2014).

The osmoregulatory role of AVT/AVP is related to maintenance of constant water and ion levels across vertebrates (Warne et al., 2002). In the apical membranes of the kidney tubule, AVP stimulates Na^+ transport by activation of Na^+ channels (Mordasini et al., 2005; Schafer et al., 1990). In human bronchial epithelial cells, AVP stimulates Cl^- and fluid secretion via a NPPB (5-Nitro-2-[3-phenylpropylamino] benzoic acid)-sensitive mechanism (Bernard et al., 2005). Additionally, AVP modifies Na^+ and Cl^- absorption in the mouse kidney through a Na-K-2Cl (NKCC) co-transporter (Hebert and Andreoli, 1984; Sun et al., 1991), likely by recruitment of co-transporter proteins to the apical membrane (Molony et al., 1987). In addition, AVP stimulates net Na^+ and Cl^- transport in the abdominal skin of amphibians such as *Hyla japonica* and *Rana nigromaculata* (Yamada et al., 2008).

The involvement of AVT in fish ion regulation seems to parallel functions of AVP described in mammals (Balment et al., 2006; Kulczykowska, 1997, 2001; Warne and Balment, 1995). Thus, AVT decreased urine output in trunk kidney preparations of rainbow trout, *Oncorhynchus mykiss* (Amer and Brown, 1995; Warne et al., 2002) and dogfish, *Scyliorhinus canicula* (Wells et al., 2002). Additionally, intra-cerebro-ventricular injections of AVT cause a reduction in water intake in seawater eels (Kozaka et al., 2003). In the sea bream, AVT treatment enhanced gill Na^+,K^+-ATPase activity after hyperosmotic challenge (Sangiao-Alvarellos et al., 2006). Also, we have recently shown an enhancement in absorptive pathways mediated by AVT in the regulation of a bumetanide sensitive mechanism, likely NKCC co-transporter, in the intestine of sea bream (Martos-Sitcha et al., 2013).

In order to sustain the ionic disequilibrium with the surrounding environment, marine fish are required to drink substantial amounts of seawater (Fuentes and Eddy, 1997). Drinking generates a surplus of plasma NaCl whose removal is fundamental to sustain plasma ion levels within narrow limits. The secretory process of monovalent ions (Na^+ and Cl^-) takes place in the gill chloride cells, which is mediated by a basolateral Na^+/K^+-ATPase and apical Cl^- secretion (Marshall and Grosell, 2005). Unfortunately, the heterogeneous and structurally complex anatomical organization of the gills precludes isolated studies on chloride cell function. However, the inner opercular epithelium of some fish, specially the killifish *Fundulus heteroclitus*, is rich in chloride cells and provides a proxy model system to study chloride cell function (Karnaky et al., 1977). When the membrane is removed and mounted in Ussing chambers the short circuit current is equivalent to Cl^- secretion rates (Degnan et al., 1977) and provides an accessible model to circumvent gill cell culture. In this way, the regulatory action of several endocrine/neuroendocrine factors (stimulatory actions of atriopeptin II (Scheide and Zadunaisky, 1988), as well as inhibitory actions of urotensin II (Evans et al., 2011; Marshall and Bern, 1979), nitric oxide (Evans et al., 2004) or cathecholamines (Marshall et al., 1993)) has been established using the opercular membrane of killifish.

Previous studies using a cell culture approach with pavement cells of the gill epithelium of the European sea bass (*Dicentrarchus labrax*), have demonstrated a stimulatory actions of AVT on Cl^- secretion via a DPC-sensitive mechanism, likely

cystic fibrosis transmembrane conductance regulator (Avella et al., 1999; Guibbolini and Avella, 2003). However, direct evidence of the AVT action in a chloride cell rich tissue is lacking. Therefore, the present study aimed to characterize the putative role of AVT and IT on the regulation of Cl^- secretion in the opercular epithelium of the killifish (*Fundulus heteroclitus*) and gilthead sea bream (*Sparus aurata*).

MATERIALS AND METHODS

Peptides and chemicals

Arginine vasotocin (AVT, [Arg^8]-Vasotocin acetate), isotocin (IT, [Ser^4, Ile^8]-Oxytocin), Forskolin (FK), 3-isobutyl-1-methylxanthine (IBMX), diphenylamine-2-carboxylate (DPC), Ouabain, bumetanide (Bum), SR 49059 (V1-receptor antagonist) and OPC-41061 (Tolvaptan, V2-receptor antagonist) were supplied by Sigma-Aldrich (Madrid, Spain).

Animals

Sea bream juveniles (*Sparus aurata,* 116.4 ± 3.6 g, 18.2 ± 1.1 cm) were obtained as fry from commercial sources (Cupimar S.A., Cádiz, Spain) and raised to juveniles. Killifish (*Fundulus heteroclitus,* 4.67 ± 0.15 g, 7.21 ± 0.52 cm) were collected with fish traps from Estero La Leocadia (Cádiz Bay, Spain). Fish were maintained in Ramalhete Marine Station (CCMar, University of Algarve, Faro, Portugal) with running seawater (35 p.p.t.) at a density <5 kg/m^3, 18-20 ºC and 12:12 hours light: dark photoperiod and handfed twice daily (final ration of 2% of the body weight) with commercial dry pellets (Sorgal, Portugal). Fish were food deprived for 24 h before sampling. The experiments conducted comply with the guidelines of the European Union Council (86/609/EU) for the use of laboratory animals. All animal protocols were performed under a "Group-1" license from the Direcção-Geral de Veterinária, Ministério da Agricultura, do Desenvolvimento Rural e das Pescas, Portugal.

AVT and IT receptor mRNA in sea bream operculum

Sea bream were anesthetized in seawater containing 2-phenoxyethanol (1:2000 v/v, Sigma, Madrid), sacrificed by decapitation and the inner skin of the operculum dissected out and flash-frozen in liquid-N_2. Total RNA was isolated using an Ultra-Turrax ® T8 (IKA®-Werke) from 30 mg of tissue (n=3) using the NucleoSpin®RNA II kit (Macherey-Nagel) and the on-column RNase-free DNase digestion (included in

the kit), at 37 °C for 30 min. After total RNA quality (Bioanalyzer 2100 with the RNA 6000 Nano kit, Agilent Technologies) and quantity (measured spectrophotometrically at 260 nm in a BioPhotometer Plus, Eppendorf) were confirmed, the reverse transcription was performed (qScript™ cDNA synthesis kit, Quanta BioSciences). PCR amplifications were carried out with the PerfeCTa SYBR® Green FastMix™ (Quanta BioSciences) with 10 ng of cDNA using the following temperature cycles: (95ºC, 10 min; [95ºC, 20 sec; 60ºC, 35 sec] X 35 cycles; *melting curve* [60 ºC to 95 ºC, 20 min], 95 ºC, 15 s) for AVTRs (V1a2-type, acc. no. KC195974; and V2-type, acc. no. KC960488) and ITR (acc. no. KC195973) β-actin (acc. no. X89920) amplification was used as a positive control. Negative controls were run adding sterile water instead of template. PCR products were separated in a 2% agarose gel to evaluate the presence or absence of each mRNA in sea bream opercular epithelium. PCR primer sequences used for amplification are shown in Table 1. PCR conditions for each primer pair were established in preliminary experiments in the exponential part of amplification curves for unique reaction products after establishing a relationship signal *vs*. number of cycles.

Immunohistochemistry

Sea bream and killifish were anaesthetized with 2-phenoxyethanol (1:2000 v/v), sacrificed by decapitation, the cranium was cut longitudinally and the gills and other tissue remains were removed carefully. The epithelial skins covering the opercular bone were dissected out and fixed directly by immersion in Bouin solution for 24 hours and maintained in 70 % ethanol till were processed for free-floating. After endogenous peroxidase (PO) inhibition (3 % H_2O_2 in methanol), sample permeabilization was carried out during 15 min with Tris-phosphate buffer (Tris-P, pH 7.8) (Na_2HPO_4 8.4 mM, KH_2PO4 3.5 mM, NaCl 120 mM, Trizma Base 10 mM) containing 0.2 % Tween 20, and blocked for 1 hour with Tris-P containing 10 % BSA (v/w). For chloride cells (CC) immunohistochemical localization analyses, opercular epithelia were incubated with the rabbit anti-alpha subunit Na^+,K^+-ATPase (NKA) antibody (Ura et al., 1996) overnight at 20°C in a humid chamber. Anti-NKA was diluted 1:500 in a Tris-P containing 1 % BSA (v/w) and 0.05% Tween 20 (v/v). After extensive washing with Tris-P, epithelia were incubated with the peroxidase label anti-rabbit IgG (1:100; Jackson Immunoresearch), and the peroxidase activity was developed using DAB (Diaminobenzidine, Sigma-Aldrich, Madrid, Spain). Pictures

were obtained with a digital camera (Spot insight color, Sterling Heights, Michigan, USA.) attached to a microscope (Leitz DIAPLAN) and controlled by Spot insight V3.2 software. Immunoreactive chloride cells were counted using the ImageJ V1.42j software.

Short-circuit current in Ussing chambers

The epithelial skin covering the opercular bone was carefully dissected out as described above and transferred to fresh-gassed saline (99.7:0.3 O_2/CO_2, Table 2 for species-specific composition). Epithelia were overlaid onto a thin bore polythene net, protected between 2 parafilm gaskets and pinned over the circular aperture of a tissue holder with the perimeter area lightly greased to minimize tissue edge damage (sea bream: P2413, 0.71 cm^2; killifish: P2410, 0.20 cm^2, Physiological Instruments, San Diego, USA). The mounted tissue was positioned between the two halves of the Ussing chamber (P2400, Physiological Instruments, San Diego, USA) with 2 mL of gassed saline (Table 2) at 22ºC and gassed with a 99.7:0.3 O_2/CO_2 mix to provide oxygenation, good mixing by gas lift and pH control to 7.80. The preparations were left to stand for at least 60 minutes or until a steady basal measurement of bioelectrical variables was achieved. Measurement of short-circuit current (Isc, $\mu A.cm^{-2}$) was performed in symmetric conditions under voltage clamp to 0 mV. Open circuit potential (Vt, mV) and Isc were monitored by means of Ag/AgCl electrodes connected to the chambers by 3 mm bore agar bridges (1 M KCl in 3% agar). Clamping of epithelia to 0 mV and recording of Isc was performed by means of a DVC-1000 voltage clamp amplifier (WPI, Sarasota, USA), or a VCCMC2 (Physiologic Instruments, San Diego, USA). Epithelial resistance (Rt, $\Omega.cm^2$) was manually calculated (Ohm's law) using the current deflections induced by a 1 mV pulse of 3 sec every minute (Table 3).

General characterization of the bioelectrical properties of sea bream operculum was targeted with the following treatments: i) bilateral addition of Forskolin (10 µM) + IBMX (100 µM) (PKA stimulator), ii) apical addition of DPC (1 mM, blocker of the Cl^- conductive pathway), iii) and basolateral addition of Ouabain (1 mM, specific inhibitor of Na^+,K^+-ATPase). To assess the Cl^- dependence of Isc, the effect of bilateral low Cl^- (6 mM) was tested and achieved with isomolar replacement of NaCl with Na-gluconate. Additionally the regulatory actions of AVT and IT in short circuit

current were tested with a single dose of AVT or IT (10^{-6} M) applied in the basolateral side.

In the killifish opercular epithelium the regulatory actions of AVT and IT on short circuit current were independently characterized in the range 10^{-9}-10^{-6} M. To test the Cl^- dependence of AVT/IT effect on Isc, hormonal stimulations were performed in the presence/absence of basolateral loop diuretic Bum (200 µM) or Cl^- free saline (Table 2). Additionally, the specific V1-receptors antagonist (SR 49059, 1 µM) and the V2-receptor antagonist (Tolvaptan, 1 µM), according with the specific blockage described in mammals, were used in combination with AVT to dissect the receptor subtype involvement on Isc regulation.

Statistics

All results are shown as mean ± standard error of the mean (mean ± SEM). After assessing homogeneity of variance and normality, statistical analysis of the data was carried out using paired Student's *t* test, one-way analysis of variance or repeated measures analysis of variance as appropriate followed by the post hoc Bonferroni test (Prism 5.0, GraphPad Software for McIntosh). The level of significance was set at $p < 0.05$ or $p < 0.01$ where noted in each case.

RESULTS

Previous to the study of the endocrine regulation of sea bream opercular epithelium by AVT and IT, we confirmed the presence of AVTR V1a2-type, AVTR V2-type and ITR mRNAs in this epithelium by RT-PCR (Figure 1). Additionally, we compared the number of chloride cells present in both species as NKA-immunoreactive cells per surface (Figure 2). In the sea bream, preparations showed 383 ± 16 cells/mm^2 whereas in the killifish chloride cells were present in significantly higher numbers, 1648 ± 32 cells/mm^2.

Basal electrophysiological properties of seawater adapted killifish and sea bream opercular epithelia are shown Table 3. Bioelectrical values here described for the opercular membrane of killifish are in keeping with those previously published in this species (Verbost et al., 1997; Evans et al., 2004). In the sea bream, opercular preparations sustained a small but stable open circuit potential of 1.03 ± 0.18 mV.

When the tissue was voltage-clamped to 0 mV, the short-circuit current (Isc) showed values of 10.04 ± 0.86 $\mu A.cm^{-2}$ and the calculated tissue resistance (Rt) was 103.91 ± 11.04 ($\Omega.cm^2$). The opercular epithelium of the sea bream relies on the basolateral Na^+,K^+-ATPase activity to sustain Isc as demonstrated by the observed inhibition >80% in the presence of basolateral Ouabain (1 mM, Figure 3). The positive current observed in this epithelium likely indicates anion secretion as revealed by current reversal when the tissue was tested at bilateral low Cl^- levels (Figure 3). This was further reinforced by the typical and significant Isc stimulation by Forskolin + IBMX and the significant reduction of Isc in the presence of the anion channel blocker DPC (apical, 1 mM, Figure 3).

In the sea bream opercular epithelium, basolateral addition of single doses of AVT (10^{-6} M) induced a homogeneous significant increase of Isc. In contrast, addition of a single dose of IT (10^{-6} M) was without effect (Figure 4). Figure 5 shows the Isc response of the killifish opercular membrane to basolateral addition of single doses of AVT (range 10^{-9} to 10^{-6}). The Isc changes presented a dual response: a short-term 3-5 min decrease followed by a sustained increase up to 1h post treatment. The immediate response showed an inverted bell-shaped effect with a maximum significant effect of --22 $\mu A.cm^{-2}$ (highest Isc decrease) at 10^{-8} M AVT, and a minimum effect at 10^{-6} M AVT. The sustained effect of AVT at 45 min post-treatment conformed to a linear dose-response increase of Isc with a threshold significant effect at a dose of 10^{-8} M AVT and maximum increase of ~20 $\mu A.cm^{-2}$ at the highest dose tested (10^{-6} M).

Unlike AVT, the effect of IT on Isc in opercular epithelium of killifish results in an immediate and sustained stimulation of the secretory pathway. The effect conformed to a typical linear dose-response increase of Isc with a threshold significant effect at a dose of 10^{-7} M IT and maximum increase of ~25 $\mu A.cm^{-2}$ at the highest dose tested (10^{-6} M, Figure 6).

The Cl^- dependence of the effects of AVT and IT on Isc in the opercular epithelium of the killifish was tested by basolateral application of 200 µM of Bum or the use of Cl^- free saline, which significantly reduced the AVT-dependent secretory Isc (Figure 7).

Administration of AVT (10^{-6} M) in combination with the specific V1-receptor antagonist (SR 49059, 1 µM) abolished the 3-5 min decrease of Isc observed in response to AVT (10^{-6} M) alone in the opercular epithelium of killifish (Figure 8). In contrast, when AVT (10^{-6} M) was administered in combination with the specific V2-receptor antagonist (Tolvaptan, 1 µM) the stimulatory action of AVT on Isc observed between 45min and 1 h was completely abolished (Figure 8).

Sea bream and killifish showed a similar relative effect of AVT and IT on Isc stimulation (Table 4), although the absolute value of effect in killifish is more than 10-fold higher than the response observed in sea bream. AVT (10^{-6} M) enhanced the secretory current pathway between 15-17%, while IT (10^{-6} M) stimulated this pathway between 5-7% in both species.

DISCUSSION

Although species-specific differences exist in transporter expression (Scott et al., 2005), the opercular epithelium of killifish is a generally accepted model to study, using electrophysiological techniques with Ussing chambers, branchial mechanisms of ion transport in marine fish (Degnan et al., 1977). Moreover, the Isc in the opercular epithelium of killifish provides a direct measure of Cl^- secretion (Degnan et al., 1977). The present study investigated the putative regulatory role of AVT and IT on Cl^- secretion exposed by modifications of Isc in the opercular membrane of killifish, a model species for ion regulation (Burnett et al., 2007), and in the sea bream, a species with high salinity tolerance (Gregorio et al., 2013; Laiz-Carrion et al., 2005), which is nonetheless unable to tolerate full-acclimatization in freshwater (Fuentes et al., 2010). Furthermore, we report clear differences in the basal properties of the opercular membrane in both species studied, likely related the number of NKA-immunoreactive cells (Figure 2)

In the opercular epithelium of sea water fish ion secretion, mainly by Cl^- movements (Degnan et al., 1977), is the single most important mechanism involved in ion transport, although the species-specific importance in this net flow is corroborated by the differences in the number of chloride cells containing the mechanism involved in the ion regulation presents in this osmoregulatory tissue. There are not previous

reports on the bioelectrical properties of the sea bream opercular membrane. Therefore, here we describe a putative Cl^- secretion pathway in basal conditions in the opercular epithelium of the sea bream. This claim is supported by: first, Isc increase in response to adenylyl cyclase activation by addition of FK (10 µM) + IBMX (100 µM) in the secretory direction; second, Isc inhibition caused by the apical addition of DPC (1 mM), an anion channel blocker; and third, the current inversion in response to bilateral decrease saline Cl^- concentrations *in vitro*. In this respect, is interestingly to remark that the lower Vt and Isc detected in Cl^- free solution could be the consequence of Ca^{2+} active uptake, which has been reported to be present in tilapia (*Oreochromis mossambicus*) and killifish (*F. heteroclitus*) opercular epithelium (Marshall et al., 1995; McCormick et al., 1992; Marshall, 2002), even in SW acclimated fish. Thus, the higher Ca^{2+} concentration in Cl^- free solution (from 1.5 mM to 5 mM Ca^{2+}) could stimulate the Ca^{2+} uptake pathways and be responsible for the current reversal here described. In addition, the basolateral Na^+/K^+-ATPase located in chloride cells generates the electrogenic potential to drive apical chloride secretion. Addition of basolateral Ouabain (1mM), which binds and inhibits the Na^+/K^+-ATPase, to sea bream opercular epithelia mounted in Ussing chambers induced a 75 % inhibition of the secretory current. It is important to note that Na^+/K^+-ATPase in the gills of the sea bream appears only in the chloride cells (Laiz-Carrion et al., 2005).

The neurohypophyseal hormones AVT and IT exert their endocrine regulation by binding to specific plasma membrane receptors. In teleosts, three different types of vasotocin receptors (AVTRs), two V1a-types and one V2-type, have been described (Lema, 2010; Lema et al., 2012). Although, recent studies suggest the presence of at least five members of this AVT receptors in different teleost fish genomes (Daza et al., 2012; Yamaguchi et al., 2012). Additionally database searches identify other unpublished sequences for AVT receptors such as the *Oryzias latipes* V1a1 (AB646237), V1a2 (AB646238) and V2 (NM_001201512), or *Cyprinodon variegatus* V1a1 (GU120189), V1a2 (GU120190) and V2 (GU120191). In the sea bream, two different AVTR (AVTR V1a2-type and AVTR V2-type) and ITR mRNAs have been reported (Martos-Sitcha et al., 2014), and all 3 are expressed in the opercular epithelium of this species (Figure 1). Thus, the occurrence of mRNA expression of these receptors in the opercular epithelium, as well as the effects observed *in vitro* by their putative ligands (see below), points to a role of AVT and IT. However, as far as

we are aware, there are not previous studies focusing on the roles of AVT and IT effects in opercular membrane of fish. Although, *in vitro* effects of AVT and/or IT have been demonstrated in several important epithelia in relation to the control of ion exchange/transport. Which include, the increase of Cl^- secretion in cultured pavement gill cells of the European sea bass *(Dicentrarchus labrax)* by AVT and/or IT (Avella et al., 1999; Guibbolini and Avella, 2003) and the increase of gill Na^+,K^+-ATPase activity after hyperosmotic challenge in the sea bream in response to AVT injection (Sangiao-Alvarellos et al., 2006). The present results showed that only AVT, and not IT, increases Cl^- secretion in Ussing chambers in sea bream operculum. The absence of response to IT could be due to its putative lower importance in this epithelium. Although, the percentage of effect observed compares well with the effects of IT in killifish opercular epithelium (see above, Table 4).

Putative circulating levels of AVT and IT reported in several teleost species, including the sea bream, are between 250 - 300 nM (AVT) or between 5.5 and 150 nM (IT) (e.g. (Kulczykowska and Stolarski, 1996; Mancera et al., 2008; Pierson et al., 1995; Rodriguez-Illamola et al., 2011)). In the opercular membrane of the killifish, AVT and IT addition were used between 1 nM to 1 µM. Dose-response curve analysis showed that in both cases the threshold significant dose for the effect of AVT and IT in the killifish operculum (between 10 and 100 nM) was in agreement with the circulating levels of both hormones described for other species. In addition, our results are in agreement with the effect described for IT in sea bass cultured gill cells (Avella et al., 1999; Guibbolini and Avella, 2003), resulting in a clear single dose-dependent effect of IT in the stimulation of Cl^- secretion.

In killifish opercular membranes, AVT showed a bi-phasic effect on Isc: i) the initial phase, where hormone addition produces a rapid (3 min after administration) and complex decrease (depending on the hormone concentration) of Isc attributable to reduced Cl^- secretion; and ii) in the second phase, of continuous AVT exposure results in a linear dose response increase of Cl^- secretion. Additionally, the modulation of Cl^- secretion mediated by AVT depends on the administered concentration, and likely relates to putative circulating hormone levels. Thus, considering the hypoosmoregulatory role of AVT (Carlson and Holmes, 1962; Haruta et al., 1991; Perrott et al., 1991), the lower plasma values of the hormone have been described in sea bream acclimated to hypoosmotic environment circa 10^{-8} M (Kleszczynska et al.,

2006). This level matches the dose of maximum inhibitory decrease in killifish Isc in response to AVT (Figure 5) and likely reflects the rapid adaptive response of Cl^- secretion when fish are challenged with low salinity. On the other hand, higher plasma values approaching to 10^{-7} M found in hyperosmotic environments, could suggest the contrary situation, where higher Cl^- secretion is required to avoid disturbances in the osmoregulatory processes. Interestingly, the stimulation of adrenergic neurons innervating the killifish opercular epithelium causes a transient decrease in Isc (Marshall et al., 1998). Thus, it is also possible that AVT firstly (3-5 min effect) stimulates a neural response mediated by alpha2-adrenoreceptors *via* an Inositol 1,4,5-triphosphate (IP_3) pathway, which is then followed by direct Cl^- secretion stimulation on the epithelial cell (45 to 60 min effect). It is important to note that IP_3 is the signaling pathway used by the AVTR V1a. New experiments with alpha-adrenergic blockers combined with AVT will be necessary to establish if the reduction of Isc in response to AVT is direct via effects on the epithelial cell or are mediated via stimulation of adrenergic neurons in the opercular membrane.

As has been previously described (Loretz, 1995), the specific Na^+-K^+-$2Cl^-$-cotransporter (NKCC) blocker Bumetanide (Bum) applied basolaterally to killifish operculum at 200 µM, completely abolished the Isc near to 0 µAmp/cm^2 (data not shown). Moreover, the same kind of effect when the real basolateral solution described for killifish is bilaterally replaced by Cl^- free solution is observed (Table 2, (Marshall et al., 2000). These results corroborate that Isc measured in basal conditions reflects Cl^- secretion. Additionally, Isc stimulation induced by both AVT and IT is significantly reduced (and nears zero) when Cl^- free solutions are used. This indicates that the effects on Isc induced by AVT and IT are Cl^- dependent, supporting the possibility that the effects of AVT and IT may be mediated by CFTR.

To characterize the double effect of AVT on Isc in the killifish opercular membrane, the blocking of selective AVTR was carried out. Electrophysiological preparations showed that AVTRs, i.e. V1a- or V2-types, may work as independent mechanisms, involved in the absorptive/anti-secretory or secretory pathways. Thus, when the opercular epithelium was treated with AVT in the presence of a specific V1-type antagonist, Cl^- secretion increased and the inhibition of Isc was absent (Figure 8). Instead, the blocking of V2-type receptor by a specific antagonist results in sustained decreases of Cl^- secretion. This indicates that the V2-type receptor is the main

integrator of the secretory pathway. Furthermore, under V2-receptor blocking, the single effect of AVT at 3 min is the result of added effects (signs considered) mediated by AVTR V1a-type alone, a response sustained up to 45 min. In contrast, in the absence of specific blockers, it is the secretory effect that prevails in the control in response to AVT. A response that results from the combined absolute effect produced individually by each type of receptor (Figure 8). Our results on AVT regulation of Isc in killifish disagree with previous experiments in cultured gill pavement cells in *Dicentrarchus labrax* where V1a-agonists, as well as AVT, stimulated Cl^- secretion (Guibbolini and Avella, 2003). This discrepancy could be a reflection of the presence of chloride cells in the complete opercular epithelium that express relatively different AVTRs in relation to pavement cells. However, this disparity might be also related to variation in osmoregulatory mechanisms between species with different degrees of euryhalinity. Additionally, it is important to note that the receptor antagonist specificity assumed in this study corresponds to the mammalian model and nothing is known about their potential binding capacity to the newly described paralogs of V1a and V2 teleost receptors (Daza et al., 2012; Yamaguchi et al., 2012).

Finally, the comparison of AVT and IT effects (1 μM) on Isc in sea bream and killifish opercular epithelia (Table 4), reveals that the relative physiological action of AVT and IT is comparable in both species, independently of the basal Isc recorded. Moreover, the effect produced by AVT is higher in terms of percentage (% over basal recorded) compared to those produced by IT. Thus suggesting a relative more important role of AVT than IT in the control of chloride cell function.

In conclusion, our results confirm an osmoregulatory role of both AVT and IT in the opercular epithelium of two different model species, e.g. the killifish and the sea bream. In addition, these results also expose the existence of a double mechanism mediated by AVT in the regulation of chloride cell function, where different receptors regulate secretion or absorption, likely depending on the osmoregulatory requirements of the fish.

ACKNOWLEDGEMENTS

The authors wish to thank Dr. C. Balmaceda-Aguilera for her excellent technical assistance in immunohistochemistry and Dr. J.B. Ortiz-Delgado for making available the microscope and digital camera. The authors would like to acknowledge the contribution of both reviewers to the manuscript.

FUNDING

JAM-S was funded by Ministry of Education (Spain) through the program "Formación de Profesorado Universitario" (Ref: AP2008-01194). This work was partially supported by Ministry of Science and Education, Spain by Project AGL2010-14876 to JMM and by the Ministry of Science and Higher Education and European Social Funds through the Portuguese National Science Foundation by Projects PTDC/MAR/104008/2008 and PTDC/MAR-BIO/3811/2012 to JF.

481 **REFERENCES**

482

483 Acher, R., 1993. Neurohypophysial peptide systems: processing machinery, hydroosmotic regulation,
484 adaptation and evolution. Regul. Pept. 45, 1-13.
485 Amer, S., Brown, J.A., 1995. Glomerular actions of arginine vasotocin in the in situ perfused trout
486 kidney. Am. J. Physiol. Regul. Integr. Comp. Physiol. 269, R775-780.
487 Avella, M., Part, P., Ehrenfeld, J., 1999. Regulation of Cl^- secretion in seawater fish (*Dicentrarchus*
488 *labrax*) gill respiratory cells in primary culture. J. Physiol. 516, 353-363.
489 Balment, R.J., Lu, W., Weybourne, E., Warne, J.M., 2006. Arginine vasotocin a key hormone in fish
490 physiology and behaviour: A review with insights from mammalian models. Gen. Comp. Endocrinol.
491 147, 9-16.
492 Bernard, K., Bogliolo, S., Ehrenfeld, J., 2005. Vasotocin and vasopressin stimulation of the chloride
493 secretion in the human bronchial epithelial cell line, 16HBE14o. British J. Pharmacol 144, 1037-1050.
494 Boselt, I., Rompler, H., Hermsdorf, T., Thor, D., Busch, W., Schulz, A., Schoneberg, T., 2009.
495 Involvement of the V2 vasopressin receptor in adaptation to limited water supply. Plos One 4 (5),
496 e5573. doi:10.1371/journal.pone.0005573.
497 Burnett, K.G., Bain, L.J., Baldwin, W.S., Callard, G.V., Cohen, S., Di Giulio, R.T., Evans, D.H.,
498 Gomez-Chiarri, M., Hahn, M.E., Hoover, C.A., Karchner, S.I., Katoh, F., MacLatchy, D.L., Marshall,
499 W.S., Meyer, J.N., Nacci, D.E., Oleksiak, M.F., Rees, B.B., Singer, T.D., Stegeman, J.J., Towle, D.W.,
500 Van Veld, P.A., Vogelbein, W.K., Whitehead, A., Winn, R.N., Crawford, D.L., 2007. Fundulus as the
501 premier teleost model in environmental biology: Opportunities for new insights using genomics. Comp.
502 Biochem. Physiol. D Genomics Proteomics. 2, 257-286.
503 Carlson, I.H., Holmes, W.N., 1962. Changes in the hormone content of the hypothalamo-hypophysial
504 system of the rainbow trout (*Salmo gairdneri*). J. Endocrinol. 24, 23-32.
505 Conklin, D.J., Smith, M.P., Olson, K.R., 1999. Pharmacological characterization of arginine vasotocin
506 vascular smooth muscle receptors in the trout (*Oncorhynchus mykiss*) in vitro. Gen. Comp. Endocrinol.
507 114, 36-46.
508 Cornett, L.E., Kirby, J.D., Vizcarra, J.A., Ellison, J.C., Thrash, J., Mayeux, P.R., Crew, M.D., Jones,
509 S.M., Ali, N., Baeyens, D.A., 2003. Molecular cloning and functional characterization of a vasotocin
510 receptor subtype expressed in the pituitary gland of the domestic chicken (*Gallus domesticus*): avian
511 homolog of the mammalian V1b-vasopressin receptor. Regul. Peptides. 110, 231-239.
512 Daza, D.O., Lewicka, M., Larhammar, D., 2012. The oxytocin/vasopressin receptor family has at least
513 five members in the gnathostome lineage, including two distinct V2 subtypes. Gen. Comp. Endocrinol.
514 175, 135-143.
515 Degnan, K.J., Karnaky, K.J., Zadunaisky, J.A., 1977. Active chloride transport in invitro opercular skin
516 of a teleost (*Fundulus heteroclitus*), a gill-like epithelium rich in chloride cells. J. Physiol-London. 271,
517 155-191.
518 Evans, D.H., Hyndman, K.A., Cornwell, E., Buchanan, P., 2011. Urotensin II and its receptor in the
519 killifish gill: regulators of NaCl extrusion. J. Exp. Biol. 214, 3985-3991.
520 Evans, D.H., Rose, R.E., Roeser, J.M., Stidham, J.D., 2004. NaCl transport across the opercular
521 epithelium of *Fundulus heteroclitus* is inhibited by an endothelin to NO, superoxide, and prostanoid
522 signaling axis. Am. J. Physiol. Regul. Integr. Comp. Physiol.286, R560-568.
523 Fuentes, J., Brinca, L., Guerreiro, P.M., Power, D.M., 2010. PRL and GH synthesis and release from
524 the sea bream (*Sparus auratus* L.) pituitary gland in vitro in response to osmotic challenge. Gen.
525 Comp. Endocrinol. 168, 95-102.
526 Fuentes, J., Eddy, F.B., 1997. Drinking in freshwater, euryhaline and marine teleost fish, in: N. Hazon,
527 F.B. Eddy, G. Flik (Eds.), Ionic regulation in animals. Springer-Verlag, Heidelberg, 135-149.
528 Fuentes, J., Figueiredo, J., Power, D.M., Canario, A.V.M., 2006. Parathyroid hormone-related protein
529 regulates intestinal calcium transport in sea bream (*Sparus auratus*). Am. J. Physiol. Regul. Integr.
530 Comp. Physiol. 291, R1499-R1506.
531 Gregorio, S.F., Carvalho, E.S., Encarnacao, S., Wilson, J.M., Power, D.M., Canario, A.V., Fuentes, J.,
532 2013. Adaptation to different salinities exposes functional specialization in the intestine of the sea
533 bream (*Sparus aurata* L.). J. Exp. Biol. 216, 470-479.
534 Guibbolini, M.E., Avella, M., 2003. Neurohypophysial hormone regulation of Cl^- secretion:
535 Physiological evidence for V1-type receptors in sea bass gill respiratory cells in culture. J. Endocrinol.
536 176, 111-119.
537 Haruta, K., Yamashita, T., Kawashima, S., 1991. Changes in arginine vasotocin content in the pituitary
538 of the Medaka (*Oryzias latipes*) during osmotic stress. Gen. Comp. Endocrinol 83, 327-336.

539 Hasunuma, I., Toyoda, F., Kadono, Y., Yamamoto, K., Namiki, H., Kikuyama, S., 2010. Localization
540 of three types of arginine vasotocin receptors in the brain and pituitary of the newt *Cynops*
541 *pyrrhogaster*. Cell Tissue Res. 342, 437-457.
542 Hausmann, H., Meyerhof, W., Zwiers, H., Lederis, K., Richter, D., 1995. Teleost isotocin receptor:
543 structure, functional expression, mRNA distribution and phylogeny. FEBS Lett 370, 227-230.
544 Hebert, S.C., Andreoli, T.E., 1984. Control of NaCl transport in the thick ascending limb. Am. J.
545 Physiol. Renal Fluid. Electrolyte Physiol. 246, F745-756.
546 Jurkevich, A., Berghman, L.R., Cornett, L.E., Kuenzel, W.J., 2005. Characterization and
547 immunohistochemical visualization of the vasotocin VT2 receptor in the pituitary gland of the chicken,
548 *Gallus gallus*. Gen. Comp. Endocrinol. 143, 82-91.
549 Karnaky, K.J., Jr., Degnan, K.J., Zadunaisky, J.A., 1977. Chloride transport across isolated opercular
550 epithelium of killifish: a membrane rich in chloride cells. Science 195, 203-205.
551 Kleszczynska, A., Vargas-Chacoff, L., Gozdowska, M., Kalamarz, H., Martinez-Rodriguez, G.,
552 Mancera, J.M., Kulczykowska, E., 2006. Arginine vasotocin, isotocin and melatonin responses
553 following acclimation of gilthead sea bream (*Sparus aurata*) to different environmental salinities.
554 Comp. Biochem. Physiol. A Mol. Integr. Physiol. 145, 268-273.
555 Konno, N., Hyodo, S., Yamaguchi, Y., Kaiya, H., Miyazato, M., Matsuda, K., Uchiyama, M., 2009.
556 African lungfish, *Protopterus annectens*, possess an arginine vasotocin receptor homologous to the
557 tetrapod V2-type receptor. J. Exp. Biol. 212, 2183-2193.
558 Kozaka, T., Fujii, Y., Ando, M., 2003. Central effects of various ligands on drinking behavior in eels
559 acclimated to seawater. J. Exp. Biol. 206, 687-692.
560 Kulczykowska, E., 1997. Response of circulating arginine vasotocin and isotocin to rapid osmotic
561 challenge in rainbow trout. Comp. Biochem. Physiol. A Mol. Integr. Physiol. 118, 773-778.
562 Kulczykowska, E., 2001. Responses of circulating arginine vasotocin, isotocin, and melatonin to
563 osmotic and disturbance stress in rainbow trout (*Oncorhynchus mykiss*). Fish Physiol. Biochem. 24,
564 201-206.
565 Kulczykowska, E., 2007. Arginine vasotocin and isotocin: towards their role in fish osmoregulation. In:
566 Fish Osmoregulation. Baldisserotto, B., Mancera Romero J.M., and Kapoor, B.G. (Eds.). Science
567 Publisher, Enfield (NH), 151-176.
568 Kulczykowska, E., Stolarski, J., 1996. Diurnal changes in plasma arginine vasotocin and isotocin in
569 rainbow trout adapted to fresh water and brackish Baltic water. Gen. Comp. Endocrinol. 104, 197-202.
570 Laiz-Carrion, R., Guerreiro, P.M., Fuentes, J., Canario, A.V., Martin Del Rio, M.P., Mancera, J.M.,
571 2005. Branchial osmoregulatory response to salinity in the gilthead sea bream, *Sparus auratus*. J. Exp.
572 Zool. A Comp. Exp. Biol. 303, 563-576.
573 Lema, S.C., 2010. Identification of multiple vasotocin receptor cDNAs in teleost fish: Sequences,
574 phylogenetic analysis, sites of expression, and regulation in the hypothalamus and gill in response to
575 hyperosmotic challenge. Mol. Cell. Endocrinol. 321, 215-230.
576 Lema, S.C., Slane, M.A., Salvesen, K.E., Godwin, J., 2012. Variation in gene transcript profiles of two
577 V1a-type arginine vasotocin receptors among sexual phases of bluehead wrasse (*Thalassoma*
578 *bifasciatum*). Gen. Comp. Endocrinol. 179, 451-464.
579 Loretz, C.A., 1995. 2 Electrophysiology of ion transport in teleost intestinal cells. In: Wood, C.M.,
580 Shuttleworth, T.J. (eds). Cellular and molecular approaches to fish ionic regulation, Fish physiology
581 Vol. 14 Academic Press, San Diego, pp 25-56.
582 Mahlmann, S., Meyerhof, W., Hausmann, H., Heierhorst, J., Schonrock, C., Zwiers, H., Lederis, K.,
583 Richter, D., 1994. Structure, function, and phylogeny of [Arg8]vasotocin receptors from teleost fish
584 and toad. Proc. Natl. Acad. Sci. USA. 91, 1342-1345.
585 Mancera, J.M., Vargas-Chacoff, L., García-Lopez, A., Kleszczynska, A., Kalamarz, H., Martínez-
586 Rodríguez, G., Kulczykowska, E., 2008. High density and food deprivation affect arginine vasotocin,
587 isotocin and melatonin in gilthead sea bream (*Sparus auratus*). Comp. Biochem. Physiol. A Mol.
588 Integr. Physiol. 149, 92-97.
589 Marshall, W.S., Bern, H.A., 1979. Teleostean urophysis: urotensin II and ion transport across the
590 isolated skin of a marine teleost. Science 204, 519-521.
591 Marshall, W.S., Bryson, S.E., Garg, D., 1993. Alpha-2-adrenergic inhibition of Cl^- transport by
592 opercular epithelium is mediated by intracellular Ca^{2+}. Proc. Natl. Acad. Sci. USA. 90, 5504-5508.
593 Marshall, W.S., Bryson, S.E., Burghardt, J.S., Verbost, P.M., 1995. Ca^{2+} transport by the opercular
594 epithelium of the freshwater-adapted euryhaline teleost *Fundulus heteroclitus*. J. Comp. Physiol. B
595 Biochem. Mol. Biol. 165, 268–277.
596 Marshall, W.S., Duquesnay, R.M., Gillis, J.M., Bryson, S.E., Liedtke, C.M., 1998. Neural modulation
597 of salt secretion in teleost opercular epithelium by α2-adrenergic receptors and inositol 1,4,5-
598 trisphospate. J. Exp. Biol. 201, 1959-1965.

599 Marshall, W.S., Bryson, S.E., Luby, T., 2000. Control of epithelial Cl(-) secretion by basolateral
600 osmolality in the euryhaline teleost *Fundulus heteroclitus*. J. Exp. Biol. 203, 1897-1905.
601 Marshall, W.S., 2002. Na^+, Cl^-, Ca^{2+} and Zn^{2+} transport by fish gills: retrospective review and
602 prospective synthesis. J. Exp. Zool. 293, 264-283.
603 Marshall, W.S., Grosell, M., 2005. Ion transport, osmoregulation and acid-base balance. In: Evans,
604 D.H., Claiborne, J.B. (Eds.) Physiology of Fishes, vol. 3. CRC Press, Boca Raton (FL), 177-230.
605 Martos-Sitcha, J.A., Fuentes, J., Mancera, J.M., Martínez-Rodríguez, G., 2014. Variations in the
606 expression of vasotocin and isotocin receptor genes in the gilthead sea bream *Sparus aurata* during
607 different osmotic challenges. Gen. Comp. Endocrinol. 197, 5-17.
608 Martos-Sitcha, J.A., Gregorio, S.F., Carvalho, E.S., Canario, A.V., Power, D.M., Mancera, J.M.,
609 Martínez-Rodríguez, G., Fuentes, J., 2013. AVT is involved in the regulation of ion transport in the
610 intestine of the sea bream (*Sparus aurata*). Gen. Comp. Endocrinol. 193, 221-228.
611 McCormick, S.D., Hasegawa, S., Hirano, T., 1992. Calcium uptake in the skin of a freshwater teleost.
612 Proc. Nat. Acad. Sci. USA. 89, 3635–3638.
613 Molony, D.A., Reeves, W.B., Hebert, S.C., Andreoli, T.E., 1987. ADH increases apical Na^+, K^+, $2Cl^-$
614 entry in mouse medullary thick ascending limbs of Henle. Am. J. Physiol. Renal Fluid. Electrolyte
615 Physiol. 252, F177-187.
616 Mordasini, D., Bustamante, M., Rousselot, M., Martin, P.Y., Hasler, U., Féraille, E., 2005. Stimulation
617 of Na^+ transport by AVP is independent of PKA phosphorylation of the Na-K-ATPase in collecting
618 duct principal cells. Am. J. Physiol. Renal Fluid. Electrolyte Physiol. 289, F1031-F1039.
619 Perrott, M.N., Carrick, S., Balment, R.J., 1991. Pituitary and plasma arginine vasotocin levels in teleost
620 fish. Gen. Comp. Endocrinol. 83, 68-74.
621 Pierson, P.M., Guibbolini, M.E., Mayer-Gostan, N., Lahlou, B., 1995. ELISA measurements of
622 vasotocin and isotocin in plasma and pituitary of the rainbow trout: effect of salinity. Peptides. 16, 859-
623 865.
624 Rodríguez-Illamola, A., López Patino, M.A., Soengas, J.L., Ceinos, R.M., Míguez, J.M., 2011. Diurnal
625 rhythms in hypothalamic/pituitary AVT synthesis and secretion in rainbow trout: evidence for a
626 circadian regulation. Gen. Comp. Endocrinol. 170, 541-549.
627 Sangiao-Alvarellos, S., Polakof, S., Arjona, F.J., Kleszczynska, A., Martín del Río, M.P., Míguez,
628 Soengas, J.L., Mancera, J.M., 2006. Osmoregulatory and metabolic changes in the gilthead sea bream
629 *Sparus auratus* after arginine vasotocin (AVT) treatment. Gen. Comp. Endocrinol. 148, 348-358.
630 Schafer, J.A., Troutman, S.L., Schlatter, E., 1990. Vasopressin and mineralocorticoid increase apical
631 membrane driving force for K^+ secretion in rat CCD. Am. J. Physiol. Renal Fluid. Electrolyte Physiol.
632 258, F199-F210.
633 Scheide, J.I., Zadunaisky, J.A., 1988. Effect of atriopeptin II on isolated opercular epithelium of
634 *Fundulus heteroclitus*. Am. J. Physiol. Regul. Integr. Comp. Physiol. 254, R27-R32.
635 Scott, G.R., Claiborne, J.B., Edwards, S.L., Schulte, P.M., Wood, C.M., 2005. Gene expression after
636 freshwater transfer in gills and opercular epithelia of killifish: insight into divergent mechanisms of ion
637 transport. J. Exp. Biol. 208, 2719-2729.
638 Sun, A., Grossman, E.B., Lombardi, M., Hebert, S.C., 1991. Vasopressin alters the mechanism of
639 apical Cl^- entry from Na^+:Cl^- to Na^+:K^+:$2Cl^-$ cotransport in mouse medullary thick ascending limb. J.
640 Membr. Biol. 120, 83-94.
641 Tan, F.I., Lolait, S.J., Brownstein, M.J., Saito, N., MacLeod, V., Baeyens, D.A., Mayeux, P.R., Jones,
642 S.M., Cornett, L.E., 2000. Molecular cloning and functional characterization of a vasotocin receptor
643 subtype that is expressed in the shell gland and brain of the domestic chicken. Biol. Reprod. 62, 8-15.
644 Thibonnier, M., Auzan, C., Madhun, Z., Wilkins, P., Berti-Mattera, L., Clauser, E., 1994. Molecular
645 cloning, sequencing, and functional expression of a cDNA encoding the human V1a vasopressin
646 receptor. J. Biol. Chem. 269, 3304-3310.
647 Ura, K., Soyano, K., Omoto, N., Adachi S., Yamauchi K., 1996. Localization of Na^+,K^+-ATPase in
648 tissues of rabbit and teleosts using an antiserum directed against a partial sequence of the alpha-
649 subunit. Zoolog. Sci. 13, 219-227.
650 ing, sequencing, and functional expr
651 Verbost, P.M., Bryson, S.E., Bonga, S.E., Marshall, W.S., 1997. Na(+)-dependent Ca^{2+} uptake in
652 isolated opercular epithelium of *Fundulus heteroclitus*. J. Comp. Physiol. B. 167, 205-212.
653 Warne, J.M., Balment, R.J., 1995. Effect of acute manipulation of blood volume and osmolality on
654 plasma [AVT] in seawater flounder. Am. J. Physiol. Regul. Integr. Comp. Physiol. 269, R1107-R1112.
655 Warne, J.M., Harding, K.E., Balment, R.J., 2002. Neurohypophysial hormones and renal function in
656 fish and mammals. Comp. Biochem. Physiol. B Biochem. Mol. Biol. 132, 231-237.

Wells, A., Anderson, W.G., Hazon, N., 2002. Development of an in situ perfused kidney preparation for elasmobranch fish: Action of arginine vasotocin. Am. J. Physiol. Regul. Integr. Comp. Physiol. 282, R1636-R1642.

Yamada, T., Nishio, T., Sano, Y., Kawago, K., Matsuda, K., Uchiyama, M., 2008. Effects of arginine vasotocin and vasopressin receptor antagonists on Na^+ and Cl^- transport in the isolated skin of two frog species, *Hyla japonica* and *Rana nigromaculata*. Gen. Comp. Endocrinol. 157, 63-69.

Yamaguchi, Y., Kaiya, H., Konno, N., Iwata, M., Miyazato, M., Uchiyama, M., Bell, J.D., Toop, T., Donald, J.A., Brenner, S., Venkatesh, B., Hyodo, S., 2012. The fifth neurohypophysial hormone receptor is structurally related to the V2-type receptor but functional similar to V1-type receptors. Gen. Comp. Endocrinol. 178, 519-528.

668 **TABLES**

669

670 **Table 1.** Specific primer sequences used for mRNA expression of AVTRs (V1a2-
671 type, acc. no. KC195974; and V2-type, acc. no. KC960488), ITR (acc. no.
672 KC195973) and β-actin (acc. no. X89920) in the opercular epithelium of the sea
673 bream.

Primer	Nucleotide sequence	Amplicon (bp)
AVTR-V1a2$_{Fw}$	5'-GACAGCCGCAAGTGATCAAG-3'	203
AVTR-V1a2$_{Rv}$	5'-CCCGACCGCACACCCCCTGGCT-3'	
AVTR-V2$_{Fw}$	5'-ATCACAGTCCTTGCATTGGTG-3'	120
AVTR-V2$_{Rv}$	5'-GCACAGGTTGACCATGAACAC-3'	
ITR$_{Fw}$	5'-GGAGGATCGTTTTAAAGACATGG-3'	120
ITR$_{Rv}$	5'-TGTTGTCTCCCTGTCAGATTTTC-3'	
β-actin$_{Fw}$	5'-TCTTCCAGCCATCCTTCCTCG-3'	108
β-actin$_{Rv}$	5'-TGTTGGCATACAGGTCCTTACGG-3'	

674

675

676 **Table 2.** Saline compositions for Ussing chamber experiments with the sea bream and
677 killifish opercular membrane. All solutions were adjusted to pH of 7.80 at 22 ºC and
678 gassed with 99.7:0.3 % O_2/CO_2.
679

mM	Sea bream (Fuentes et al., 2006)		Killifish (Marshall et al., 2000)	
	Normal	Low Cl^-	Normal	Cl^- Free
NaCl	160	-	160	-
Na- gluconate	-	160	-	160
$MgSO_4$	1	1	0.93	0.93
NaH_2PO_4	2	2	3	3
$CaCl_2$	1.5	1.5	1.5	-
Ca-gluconate	-	-	-	5
$NaHCO_3$	5	5	17.85	17.85
KCl	3	3	3	-
K-gluconate	-	-	-	3
Glucose	5.5	5.5	5.5	5.5
HEPES	5	5	5	5

680
681

682 **Table 3.** Bioelectrical properties of opercular epithelia of seawater-adapted killifish
683 and sea bream mounted in Ussing chambers.
684

Parameters	Sea bream (n = 29)	Killifish (n = 25)
Vt (Open circuit, mV)	1.03 ± 0.18	7.01 ± 0.56
Isc ($\mu A.cm^{-2}$)	10.04 ± 0.86*	125.86 ± 12.99*
Rt ($\Omega.cm^2$)	103.91 ± 11.04	72.59 ± 6.17

685 * Positive currents indicate secretion of anions
686
687
688
689
690
691
692
693
694 **Table 4**. Comparative effect of single doses of basolateral AVT or IT (10^{-6} M) shown
695 as % increase from basal in opercular membrane short circuit current (Isc) in the sea
696 bream and the killifish.
697

Hormone	Sea bream *(n = 5-6)*	Killifish *(n = 5-6)*
AVT	17.18 ± 2.75	15.05 ± 2.01
IT	6.73 ± 1.29	5.46 ± 1.97

698
699

FIGURE LEGENDS

Figure 1. mRNA expression of the AVTR V1a2 (acc. no. KC195974); AVTR V2 type, (acc. no. KC960488),and ITR (acc. no. KC195973). in the opercular epithelium of the sea bream. PCR products were analyzed by electrophoresis on a 2% agarose gel stained with GelRed. β-actin (acc. no. X89920) was used as a positive control, and sterile water as a negative control (- Control).

Figure 2. Density of NKA immunoreactive cells in the opercular epithelium of sea bream and killifish adapted to seawater. Each column represents the average + SEM of 6 individuals. Asterisks represent significant differences between species ($p<0.01$, Student t-test).

Figure 3. Short circuit current (Isc, μAmp/cm^2) in the opercular epithelium of the sea bream in response to addition of the following chemicals: A: FK + IBMX (10 μM + 100 μM, bilateral); B: DPC (apical, 1 mM); C: Ouabain (basolateral, 1 mM); D: Low Cl^- (bilateral, see Table 2). Each column represents the average ± SEM of 6-7 individuals. Asterisks represent significant differences from basal values ($p<0.05$, Student t-test).

Figure 4. Original trace of short circuit current (Isc, μAmp/cm^2) in response to AVT (A) or IT (B) in the opercular epithelium of the sea bream mounted in Ussing chambers; vertical current deflections are generated by 1 mV pulses to calculate Rt. Effects of basolateral AVT (C) or IT (D) 10^{-6} M on Isc (μAmp.cm^{-2}). In C, D each column represents the average ± SEM of 5-6 individuals. Asterisks represent significant differences from basal values ($p<0.05$, Student t-test).

Figure 5. Variation of short circuit current (ΔIsc, μAmp/cm^2) in response to basolateral addition of AVT in the opercular epithelium of killifish mounted in Ussing chambers. A: Original trace of the effect of AVT; vertical current deflections are generated by 1 mV pulses; B and C represent the time point from where ΔIsc values were retrieved to generate the corresponding figures. B: dose-response 10^{-9} to 10^{-6} M after 3-5 minutes post-treatment in the absorptive pathway. C: dose-response effect of 10^{-9} to 10^{-6} M after 45 minutes post-treatment in the secretory pathways. In B and C

each column represents the average ± SEM of 5 individuals. In C Asterisks represent significant differences from basal values ($p<0.01$, One-way ANOVA).

Figure 6. Variation of short circuit current (ΔIsc, μAmp/cm^2) in response to basolateral addition of IT in the opercular epithelium of killifish mounted in Ussing chambers. A: original trace in response of IT 10^{-6} M (A); vertical current deflections are generated by -1 mV pulses to calculate Rt. B: dose-response (10^{-9} to 10^{-6} M) effects after 45 minutes post-treatment. Each point represents the average ± SEM of 5 individuals. Asterisks represent significant differences from basal values ($p<0.01$, One-way ANOVA).

Figure 7. AVT (A) or IT (B) -dependent short circuit current variation (ΔIsc, μAmp/cm^2) in opercular epithelium of the killifish mounted in Ussing chamber. Basolateral addition of hormones was tested alone (AVT, IT; 10^{-6} M) or after chloride secretion inhibition by basolateral Bumetanide (Bum, 200 μM) treatment or Cl^- free solution. Results are shown as mean ± SEM (n=6). Asterisks represent significant differences from AVT alone ($p<0.01$, One-way ANOVA).

Figure 8. Original trace of short circuit current (Isc, μAmp/cm^{22}) in response to basolateral AVT (10^{-6} M) in the opercular epithelium of killifish mounted in Ussing chambers after V1 (A) or V2 (B) receptor antagonist (1 μM) treatment; vertical current deflections are generated by 1 mV pulses to calculate Rt. In C, effects of basolateral AVT (10^{-6} M) addition on variation of short circuit current (ΔIsc, μAmp/cm^2) after V1 (A) or V2 (B) receptor antagonist (1 μM) treatment. Each point represents the average + SEM of 5 individuals.

760 **Figure 1. Martos-Sitcha *et al.***

761

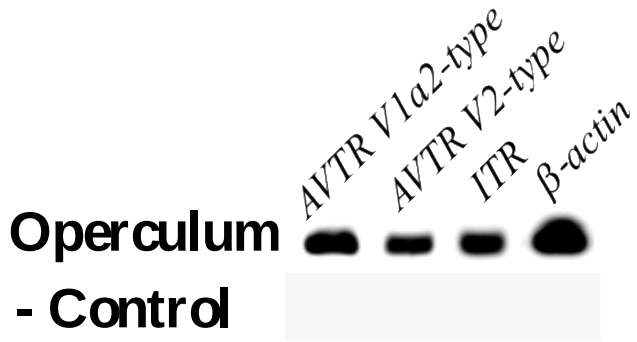

762

763

764 **Figure 2. Martos-Sitcha *et al.***

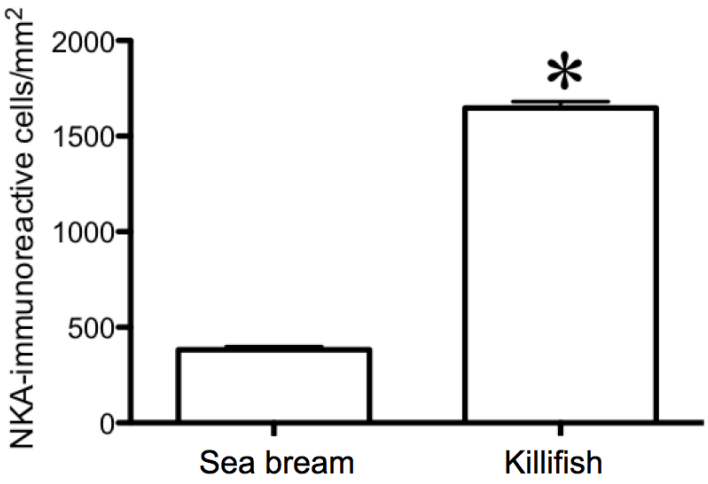

765 **Figure 3. Martos-Sitcha *et al.***

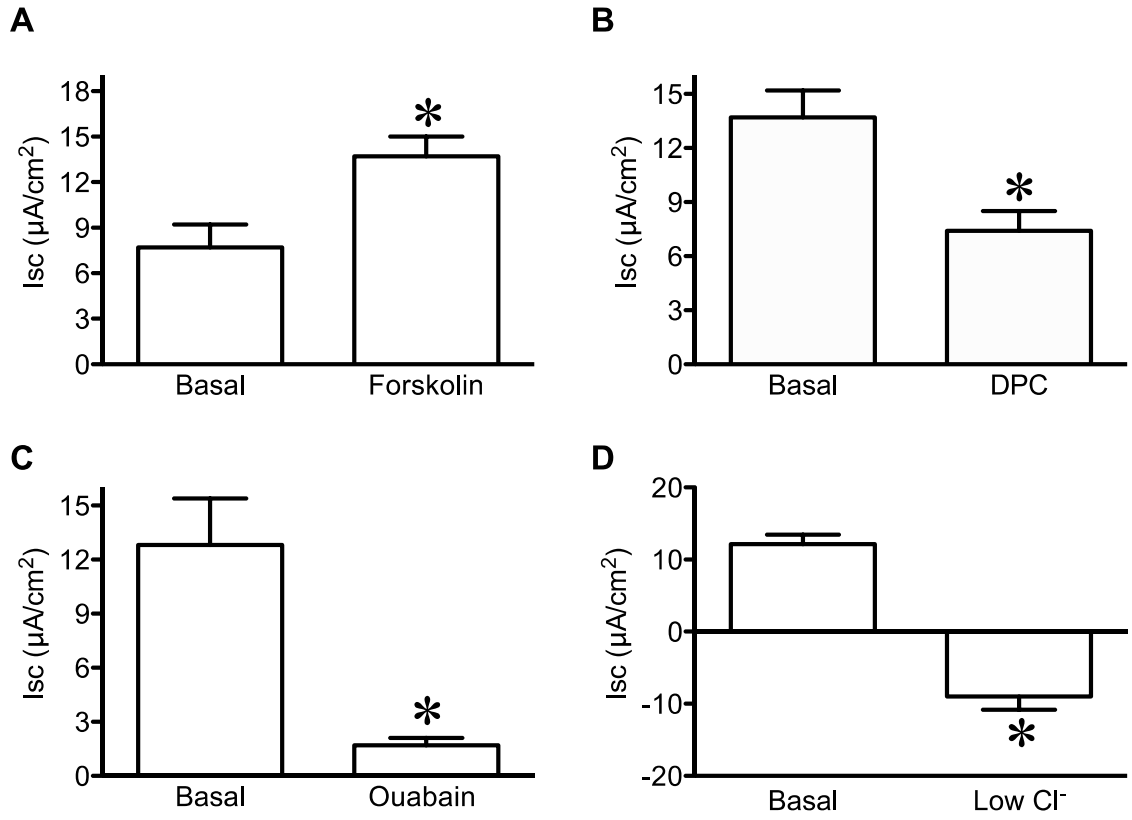

766 **Figure 4. Martos-Sitcha *et al.***

767

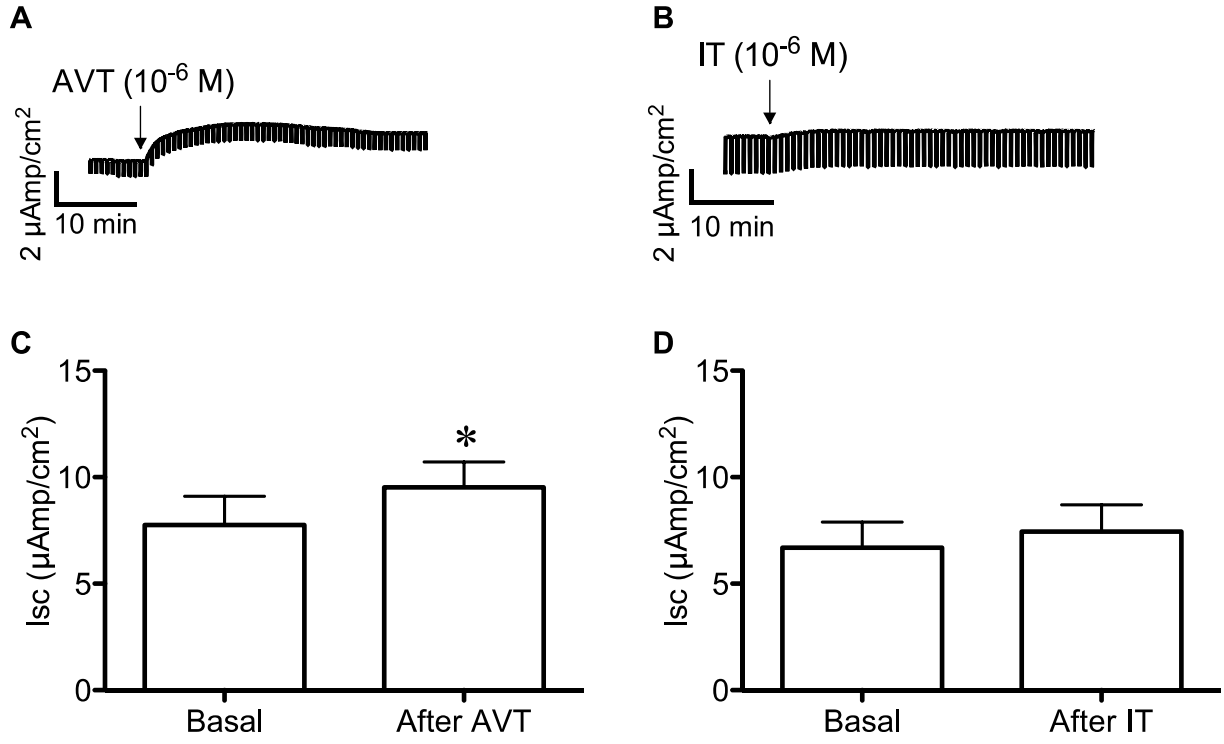

768 **Figure 5. Martos-Sitcha *et al.***

769

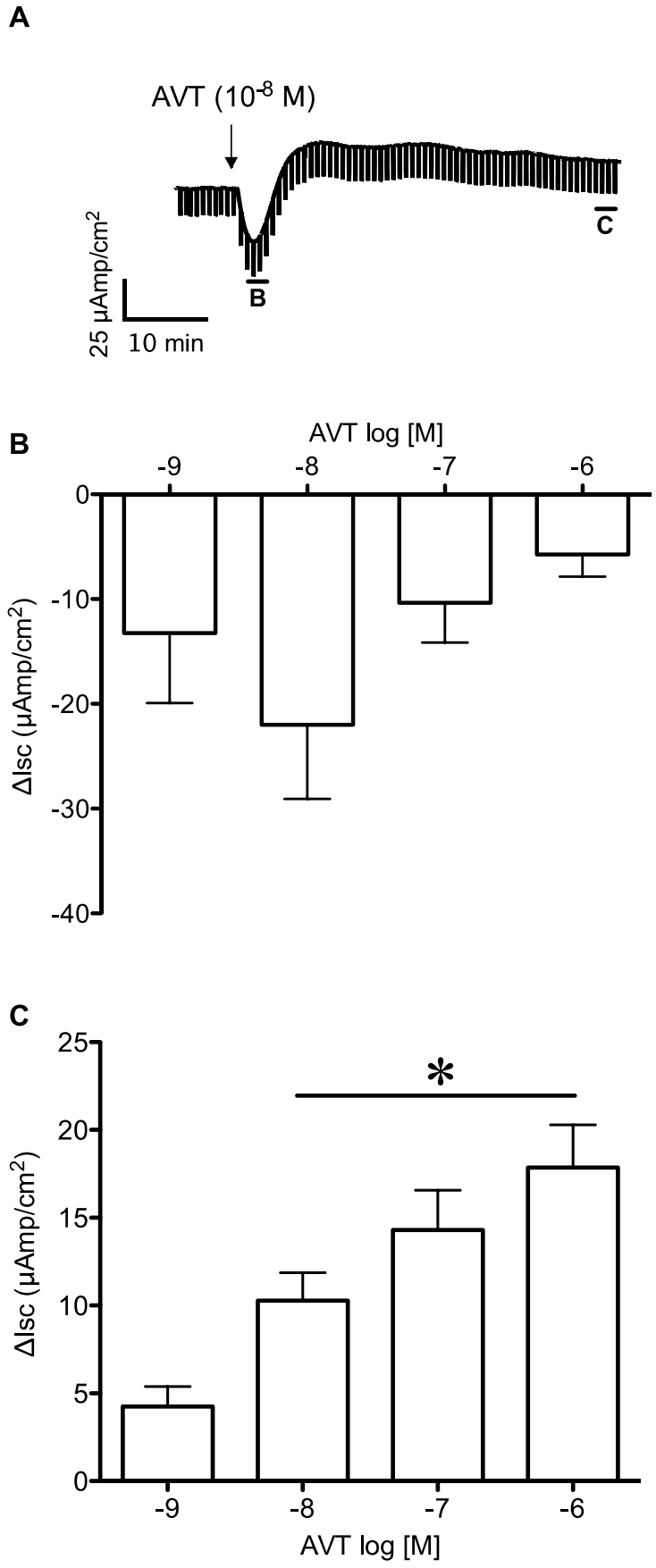

770 **Figure 6**. **Martos-Sitcha *et al.***

771

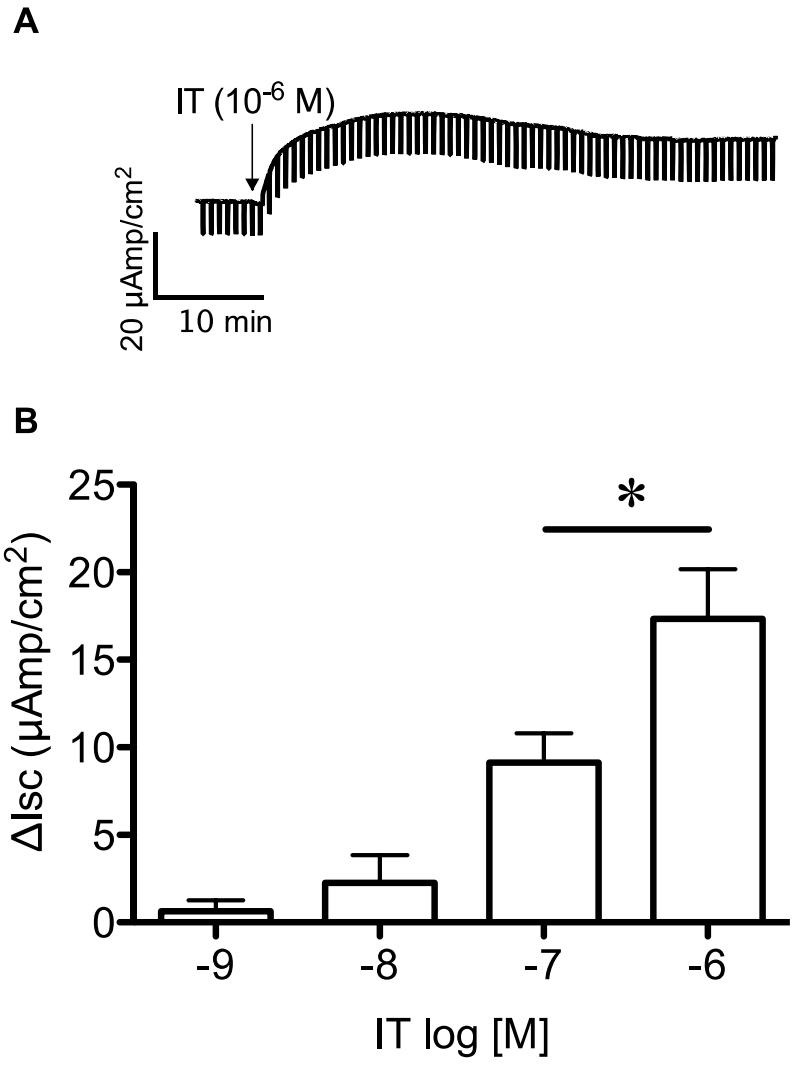

772 **Figure 7. Martos-Sitcha *et al.***

773

774

775

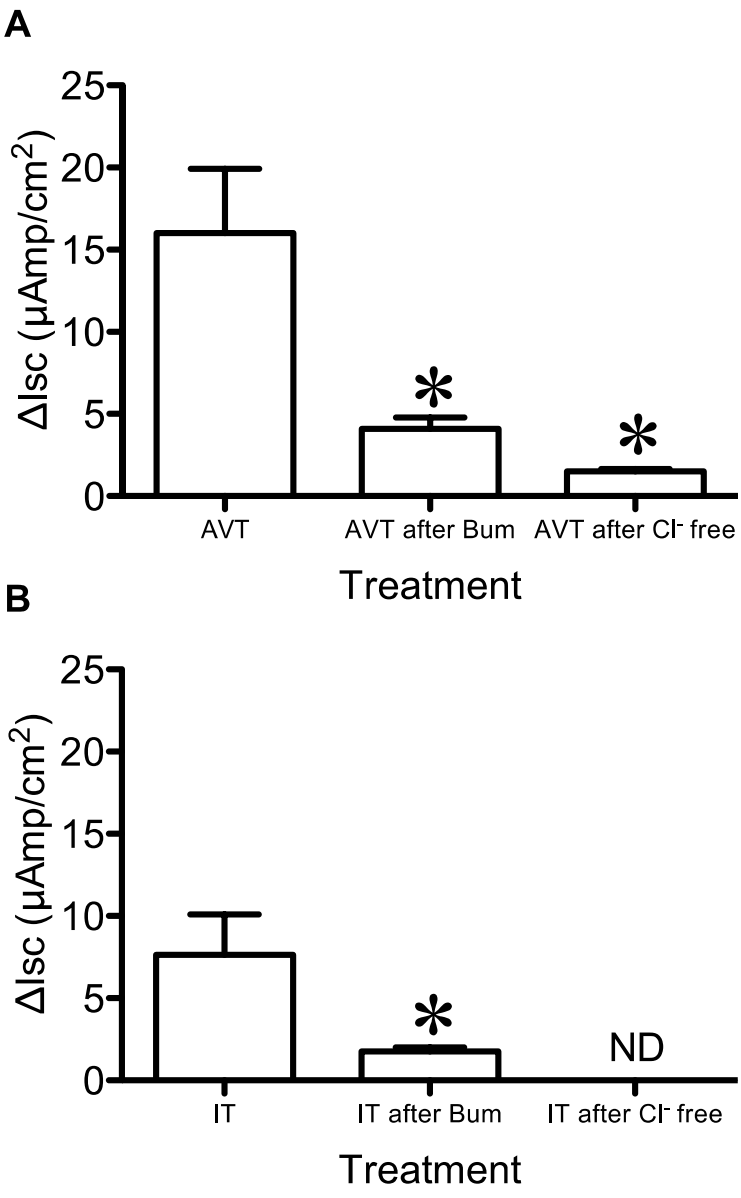

776 **Figure 8**. **Martos-Sitcha *et al.***